



Three-dimensional Green's functions in anisotropic piezoelectric bimetals

E. Pan^{a,*}, F.G. Yuan^b

^a Structures Technology, Inc., 543 Keisler Dr., Suite 204, Cary, NC 27511, USA

^b Department of Mechanical and Aerospace Engineering, North Carolina State University, Raleigh, NC 27695, USA

Received 12 July 1999; received in revised form 8 December 1999; accepted 15 December 1999

Abstract

In this paper, a recently proposed method by E. Pan and F.G. Yuan (Int. J. Solids Struct., 2000) for the calculation of the elastic bimaterial Green's functions is extended to the analysis of three-dimensional Green's functions for anisotropic piezoelectric bimetals. The method is based on the Stroh formalism and two-dimensional Fourier transforms in combination with Mindlin's superposition method. We first derive Green's functions in exact form in the Fourier transform domain. When inverting the Fourier transform, a polar coordinate transform is introduced so that the radial integral from 0 to $+\infty$ can be carried out exactly. Therefore, the bimaterial Green's functions in the physical domain are derived as a sum of a full-space Green's function and a complementary part. While the full-space Green's function is in an explicit form, as derived recently by E. Pan and F. Tonon (Int. J. Solids Struct., 37 (2000): 943–958), the complementary part is expressed in terms of simple regular line integrals over $[0, 2\pi]$ that are suitable for standard numerical integration. Furthermore, the present bimaterial Green's functions can be reduced to the special cases such as half-space, surface, interfacial, and full-space Green's functions. Uncoupled solutions for the purely elastic and purely electric case can also be simply obtained by setting the piezoelectric coefficients equal to zero. Numerical examples for Green's functions are given for both half-space and bimaterial cases with transversely isotropic and anisotropic material properties to verify the applicability of the technique. Certain interesting features associated with these Green's functions are observed and discussed, as related to the selected material properties. © 2000 Elsevier Science Ltd. All rights reserved.

1. Introduction

Fundamental three-dimensional Green's functions are of great interest to the solution of inclusion problems and of the boundary integral equations. Under the assumption of linear elastic

* Corresponding author. Tel.: +1-919-816-0434; fax: +1-919-816-0438.
E-mail address: pan@ipass.net (E. Pan).

deformation, various three-dimensional Green's functions have been derived. A brief review can be found in a recent paper by Pan and Yuan [1] where they derived the three-dimensional Green's functions in anisotropic elastic bimetals in terms of a regular line integral over $[0, 2\pi]$.

Because of their inherent coupling between mechanical and electric behavior, piezoelectric materials are now being widely applied to different engineering technologies. This stimulates various theoretical studies on piezoelectric materials, in particular, on Green's functions in such materials. It is well known that under the assumption of two-dimensional deformation, the exact closed-form Green's functions in anisotropic piezoelectric infinite plane, half plane, and bimaterial full plane can be derived based on either the Stroh formalism or the direct complex function method [3–5]. With these 2D Green's functions, fracture mechanics problems in anisotropic piezoelectric media can then be easily analyzed using the single-domain boundary-element formulation [5]. For the corresponding three-dimensional deformation, the anisotropic piezoelectric Green's functions are unlikely to obtain in an exact closed form, with the exception of transverse isotropy. For the case of transversely isotropic piezoelectric materials, Green's functions in an infinite space, a half space and bimetals have been derived recently by Dunn and Wienecke [6,7] and Ding et al. [8–10]. Therefore, for the general anisotropic piezoelectric 3D case, the numerical integral formulation developed by Barnett [11] was applied to calculate the 3D full-space Green's functions, as extensively studied by Chen [12] and Chen and Lin [13]. Recently Pan and Tonon [2] derived the 3D full-space Green's functions in terms of the eigenvalues, without numerical integration being involved. So far, however, 3D Green's functions are not available for either general anisotropic piezoelectric half-space or general anisotropic piezoelectric bimetals.

Stimulated by a very recent work of Pan and Yuan [1] where the 3D Green's functions in anisotropic elastic bimetals using the Stroh formalism and two-dimensional Fourier transform in combination with Mindlin's superposition method [14] have been derived, this paper presents the 3D Green's functions in anisotropic piezoelectric half space and bimetals. Here we further demonstrate that the Stroh formalism can equally and successfully be applied to the three-dimensional anisotropic piezoelectric bimetals.

Numerical examples are also presented for both half-space and bimaterial cases with transversely isotropic and anisotropic material properties. The responses of Green's functions for different half-space and bimaterial cases due to different types of point sources are discussed. It is observed that some of these Green's functions are material-dependent (i.e., in the source region with the same material properties, Green's functions behave similarly for both half-space and bimaterial cases), others are case-dependent (i.e., Green's functions behave similarly for a half-space case or bimaterial case despite whether the material properties are transversely isotropic or anisotropic). Another interesting feature is associated with the responses of Green's electric displacements where the electric displacements in the anisotropic region are negligible compared to those in the transversely isotropic region. This feature, however, is due to the magnitude difference of the piezoelectric and dielectric constants between the selected anisotropic and transversely isotropic materials.

2. Basic equations

Assuming a static deformation, the field equations for a linear and generally anisotropic piezoelectric solid consist of [15]:

Equilibrium equations:

$$\begin{aligned}\sigma_{ji,j} + f_i &= 0, \\ D_{i,i} - q &= 0,\end{aligned}\tag{1}$$

where σ_{ij} and D_i are the stress and electric displacement, respectively; f_i and q are the body force and electric charge, respectively. In this and the following sections, lowercase (uppercase) subscripts will always range from 1 to 3 (1 to 4). Summation over repeated lowercase (uppercase) subscripts is implied. A subscript comma denotes the partial differentiation with respect to the coordinates (i.e., x_1, x_2, x_3 or x, y, z).

Constitutive relations:

$$\begin{aligned}\sigma_{ij} &= C_{ijlm}\gamma_{lm} - e_{kji}E_k, \\ D_i &= e_{ijk}\gamma_{jk} + \varepsilon_{ij}E_j,\end{aligned}\tag{2}$$

where γ_{ij} is the strain and E_i the electric field; C_{ijlm} , e_{ijk} and ε_{ij} are the elastic moduli, the piezoelectric coefficients, and the dielectric constants, respectively. The uncoupled state (purely elastic and purely electric deformation) can be obtained by simply setting $e_{ijk} = 0$. The constants satisfy the following symmetries:

$$\begin{aligned}C_{ijlm} &= C_{jilm} = C_{lmij}, \\ e_{kji} &= e_{kij}, \\ \varepsilon_{ij} &= \varepsilon_{ji}.\end{aligned}$$

Elastic strain-displacement and electric field-potential relations:

$$\begin{aligned}\gamma_{ij} &= \frac{1}{2}(u_{i,j} + u_{j,i}), \\ E_i &= -\phi_{,i},\end{aligned}\tag{3}$$

where u_i and ϕ are the elastic displacement and electric potential, respectively.

The notation introduced by Barnett and Lothe [3] has been shown to be very convenient for the analysis of piezoelectric problems. With this notation, the elastic displacement and electric potential, the elastic strain and electric field, the stress and electric displacement, and the elastic and electric moduli (or coefficients) can be grouped together as [3,5]:

$$u_I = \begin{cases} u_i, & I = 1, 2, 3, \\ \phi, & I = 4, \end{cases}\tag{4}$$

$$\gamma_{Ij} = \begin{cases} \gamma_{ij}, & I = 1, 2, 3, \\ -E_j, & I = 4, \end{cases}\tag{5}$$

$$\sigma_{iJ} = \begin{cases} \sigma_{ij}, & J = 1, 2, 3, \\ D_i, & J = 4, \end{cases} \quad (6)$$

$$C_{iJKl} = \begin{cases} C_{ijkl}, & J, K = 1, 2, 3, \\ e_{lij}, & J = 1, 2, 3; K = 4, \\ e_{ikl}, & J = 4; K = 1, 2, 3, \\ -\varepsilon_{il}, & J = K = 4. \end{cases} \quad (7)$$

It is noted that we have kept the original symbols instead of introducing new ones since they can be easily distinguished by the range of uppercase subscripts. In terms of this shorthand notation, the constitutive relations can be unified into a single equation

$$\sigma_{iJ} = C_{iJKl} \gamma_{Kl}. \quad (8)$$

Similarly, the equilibrium equations in terms of *the extended stresses* can be recast into

$$\sigma_{iJ,i} + f_J = 0, \quad (9)$$

with f_J being defined as

$$f_J = \begin{cases} f_j, & J = 1, 2, 3, \\ -q, & J = 4. \end{cases} \quad (10)$$

It is observed that the structure of Eqs. (8) and (9) is similar to its purely elastic counterpart. Therefore, the solution method developed recently by Pan and Yuan [1] can be extended and applied to the current Green's function analysis for anisotropic piezoelectric materials. For easy reference, we will, in the following sections, use *the extended displacement* to stand for the elastic displacement and electric potential as defined in Eq. (4), and use *the extended stress* for the stress and electric displacement as defined in Eq. (6).

3. Problem description

We now consider an anisotropic piezoelectric bimaterial full space where $x_3 > 0$ and $x_3 < 0$ are occupied by materials 1 and 2, respectively (Fig. 1), with the interface being at $x_3 = 0$ plane. Without loss of generality, we assume that an extended concentrated force $\mathbf{f} = (f_1, f_2, f_3, -q)$ is applied at $(0, 0, d)$ in material 1 with $d > 0$.

The continuity conditions at the interface $x_3 = 0$ require that the extended displacement and traction vectors are continuous, i.e.,

$$\mathbf{u}_1|_{x_3=0^+} = \mathbf{u}_2|_{x_3=0^-}, \quad \mathbf{t}_1|_{x_3=0^+} = \mathbf{t}_2|_{x_3=0^-}, \quad (11)$$

where subscripts 1 and 2 denote, respectively, the material half-spaces 1 and 2; t_1 and t_2 are the extended traction vectors on $x_3 = \text{constant}$ plane with components defined as

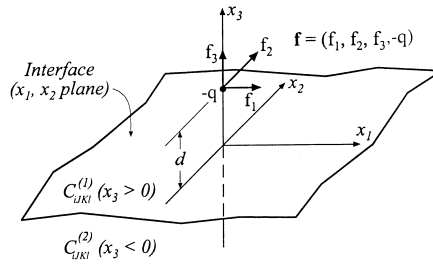


Fig. 1. An anisotropic piezoelectric bimaterial full space subjected to an extended concentrated force f applied at $(0, 0, d)$ in material 1.

$$t = (\sigma_{31}, \sigma_{32}, \sigma_{33}, D_3). \tag{12}$$

At the plane $x_3 = d$ where the extended point force is applied, the extended displacement and traction vectors satisfy the following conditions:

$$\begin{aligned} u_1|_{x_3=d^-} &= u_1|_{x_3=d^+}, \\ t_1|_{x_3=d^-} - t_1|_{x_3=d^+} &= \delta(x_1)\delta(x_2)f. \end{aligned} \tag{13}$$

It is also required that the solutions in the region of $x_3 > d$ and in the region of $x_3 < 0$ be bounded as x_3 approaches $+\infty$ and $-\infty$, respectively.

4. Stroh formalism and general solutions in the transformed domain

Similar to the purely elastic bimaterial problem [1], we introduce the two-dimensional Fourier transforms

$$\tilde{u}_K(y_1, y_2, x_3) = \int \int u_K(x_1, x_2, x_3) e^{i\mathbf{y} \cdot \mathbf{x}} dx_1 dx_2, \tag{14}$$

where $\mathbf{y} = (y_1, y_2)$ is the transform vector; \mathbf{x} denotes (x_1, x_2) , and

$$\mathbf{y} \cdot \mathbf{x} = y_1x_1 + y_2x_2.$$

In the transformed domain, Eq. (9), without the extended forces, becomes

$$C_{\alpha IK\beta} y_\alpha y_\beta \tilde{u}_K + i(C_{\alpha IK3} + C_{3IK\alpha}) y_\alpha \tilde{u}_{K,3} - C_{3IK3} \tilde{u}_{K,33} = 0, \tag{15}$$

where $\alpha, \beta = 1, 2$. Now, letting

$$\mathbf{y} = \eta \mathbf{n}, \quad \mathbf{n} = \begin{bmatrix} n_1 \\ n_2 \\ 0 \end{bmatrix} = \begin{bmatrix} \cos \theta \\ \sin \theta \\ 0 \end{bmatrix}, \quad \mathbf{m} = \begin{bmatrix} 0 \\ 0 \\ 1 \end{bmatrix}, \tag{16}$$

a general solution of Eq. (15) can then be expressed as

$$\tilde{\mathbf{u}}(y_1, y_2, x_3) = \mathbf{a} e^{-ip\eta x_3}, \quad (17)$$

with p and \mathbf{a} satisfying the following eigenrelation:

$$[\mathbf{Q} + p(\mathbf{R} + \mathbf{R}^T) + p^2 \mathbf{T}] \mathbf{a} = 0, \quad (18)$$

where

$$Q_{IK} = C_{jIKs} n_j n_s, \quad R_{IK} = C_{jIKs} n_j m_s, \quad T_{IK} = C_{jIKs} m_j m_s, \quad (19)$$

and the superscript T denotes the transpose. Eq. (18) is the eighth polynomial in p and is the piezoelectric Stroh eigenrelation in the oblique plane spanned by \mathbf{n} and \mathbf{m} defined in Eq. (16). This equation is a direct extension of the elastic Stroh eigenrelation with the sixth polynomial in p [1,3,4]. It has been shown [4,16] that the eigenvalues of Eq. (18) are either complex or purely imaginary. Once the eigenvalue problem (18) is solved, the extended displacements are obtained by Eq. (17). The extended traction vector t on the $x_3 = \text{constant}$ plane and the extended in-plane stress vector s are related to the extended displacements as

$$\begin{aligned} t &= (\sigma_{31}, \sigma_{32}, \sigma_{33}, D_3), \\ &= (C_{31KI} u_{K,l}, C_{32KI} u_{K,l}, C_{33KI} u_{K,l}, C_{34KI} u_{K,l}), \end{aligned} \quad (20)$$

$$\begin{aligned} s &\equiv (\sigma_{11}, \sigma_{12}, \sigma_{22}, D_1, D_2), \\ &= (C_{11KI} u_{K,l}, C_{12KI} u_{K,l}, C_{22KI} u_{K,l}, C_{14KI} u_{K,l}, C_{24KI} u_{K,l}). \end{aligned} \quad (21)$$

Making use of the extended displacement solution (17), the transformed extended traction and in-plane stress vectors can be found as

$$\tilde{\mathbf{t}} = -i\eta \mathbf{b} e^{-ip\eta x_3}, \quad (22)$$

$$\tilde{\mathbf{s}} = -i\eta \mathbf{c} e^{-ip\eta x_3}, \quad (23)$$

with

$$\begin{aligned} \mathbf{b} &= (\mathbf{R}^T + p\mathbf{T}) \mathbf{a} = -\frac{1}{p} (\mathbf{Q} + p\mathbf{R}) \mathbf{a}, \\ \mathbf{c} &= \mathbf{H} \mathbf{a}, \end{aligned} \quad (24)$$

where matrix \mathbf{H} is defined by

$$\mathbf{H} = \begin{bmatrix} C_{111\alpha}n_\alpha + pC_{1113} & C_{112\alpha}n_\alpha + pC_{1123} & C_{113\alpha}n_\alpha + pC_{1133} & C_{114\alpha}n_\alpha + pC_{1143} \\ C_{121\alpha}n_\alpha + pC_{1213} & C_{122\alpha}n_\alpha + pC_{1223} & C_{123\alpha}n_\alpha + pC_{1233} & C_{124\alpha}n_\alpha + pC_{1243} \\ C_{221\alpha}n_\alpha + pC_{2213} & C_{222\alpha}n_\alpha + pC_{2223} & C_{223\alpha}n_\alpha + pC_{2233} & C_{224\alpha}n_\alpha + pC_{2243} \\ C_{141\alpha}n_\alpha + pC_{1413} & C_{142\alpha}n_\alpha + pC_{1423} & C_{143\alpha}n_\alpha + pC_{1433} & C_{144\alpha}n_\alpha + pC_{1443} \\ C_{241\alpha}n_\alpha + pC_{2413} & C_{242\alpha}n_\alpha + pC_{2423} & C_{243\alpha}n_\alpha + pC_{2433} & C_{244\alpha}n_\alpha + pC_{2443} \end{bmatrix}, \quad (25)$$

with $\alpha = 1, 2$.

If p_m , \mathbf{a}_m , and \mathbf{b}_m ($m = 1, 2, \dots, 8$) are the eigenvalues and the associated eigenvectors, we let

$$\begin{aligned} \text{Im } p_J > 0, \quad p_{J+4} = \bar{p}_J, \quad \mathbf{a}_{J+4} = \bar{\mathbf{a}}_J, \quad \mathbf{b}_{J+4} = \bar{\mathbf{b}}_J \quad (J = 1, 2, 3, 4), \\ \mathbf{A} = [\mathbf{a}_1, \mathbf{a}_2, \mathbf{a}_3, \mathbf{a}_4], \quad \mathbf{B} = [\mathbf{b}_1, \mathbf{b}_2, \mathbf{b}_3, \mathbf{b}_4], \quad \mathbf{C} = [\mathbf{c}_1, \mathbf{c}_2, \mathbf{c}_3, \mathbf{c}_4, \mathbf{c}_5], \end{aligned} \quad (26)$$

where Im stands for the imaginary part and the overbar denotes the complex conjugate. Assuming that p_J are distinct, and the eigenvectors \mathbf{a}_J , and \mathbf{b}_J satisfy the following normalization relation [3]

$$\mathbf{b}_J^T \mathbf{a}_J + \mathbf{a}_J^T \mathbf{b}_J = \delta_{JJ}, \quad (27)$$

with δ_{JJ} being the Kronecker delta of 4×4 , then the general solutions of Eq. (17) in the transformed domain can be obtained by superposing eight eigensolutions of Eq. (18), i.e.,

$$\begin{aligned} \tilde{\mathbf{u}}(y_1, y_2, x_3) &= i\eta^{-1} \bar{\mathbf{A}} \langle e^{-i\bar{p}_* \eta x_3} \rangle \bar{\mathbf{q}} + i\eta^{-1} \mathbf{A} \langle e^{-ip_* \eta x_3} \rangle \mathbf{q}', \\ \tilde{\mathbf{t}}(y_1, y_2, x_3) &= \bar{\mathbf{B}} \langle e^{-i\bar{p}_* \eta x_3} \rangle \bar{\mathbf{q}} + \mathbf{B} \langle e^{-ip_* \eta x_3} \rangle \mathbf{q}', \\ \tilde{\mathbf{s}}(y_1, y_2, x_3) &= \bar{\mathbf{C}} \langle e^{-i\bar{p}_* \eta x_3} \rangle \bar{\mathbf{q}} + \mathbf{C} \langle e^{-ip_* \eta x_3} \rangle \mathbf{q}', \end{aligned} \quad (28)$$

where $\bar{\mathbf{q}}$ and \mathbf{q}' are arbitrary complex vectors to be determined and

$$\langle e^{-ip_* \eta x_3} \rangle = \text{diag}[e^{-ip_1 \eta x_3}, e^{-ip_2 \eta x_3}, e^{-ip_3 \eta x_3}, e^{-ip_4 \eta x_3}]. \quad (29)$$

It is noteworthy that, besides their obvious dependence on material properties, matrices \mathbf{A} , \mathbf{B} , \mathbf{C} , vectors $\bar{\mathbf{q}}$, \mathbf{q}' , and p_j are also functions of the unit vector \mathbf{n} .

5. Bimaterial Greens functions in the transformed domain

For the anisotropic piezoelectric bimetals, the continuity condition in Eq. (11) at the interface $x_3 = 0$ and the condition (13) at $x_3 = d$ become, in the transformed domain, as

$$\tilde{\mathbf{u}}_1|_{x_3=0^+} = \tilde{\mathbf{u}}_2|_{x_3=0^-}, \quad \tilde{\mathbf{t}}_1|_{x_3=0^+} = \tilde{\mathbf{t}}_2|_{x_3=0^-}, \quad (30)$$

and

$$\begin{aligned} \tilde{\mathbf{u}}_1|_{x_3=d^-} &= \tilde{\mathbf{u}}_1|_{x_3=d^+}, \\ \tilde{\mathbf{t}}_1|_{x_3=d^-} - \tilde{\mathbf{t}}_1|_{x_3=d^+} &= \mathbf{f}. \end{aligned} \quad (31)$$

Using these conditions as well as the requirement that the solutions should be bounded as x_3 approaches infinity, the bimaterial Green's functions in the transformed domain can be derived similarly as for the purely elastic case [1].

For $x_3 > d$ (in material 1):

$$\begin{aligned}\tilde{\mathbf{u}}_1(y_1, y_2, x_3) &= -i\eta^{-1} \bar{\mathbf{A}}_1 \langle e^{-ip_*^{(1)} \eta(x_3-d)} \rangle \bar{\mathbf{q}}_1^\infty - i\eta^{-1} \bar{\mathbf{A}}_1 \langle e^{-ip_*^{(1)} \eta x_3} \rangle \bar{\mathbf{q}}_1, \\ \tilde{\mathbf{t}}_1(y_1, y_2, x_3) &= -\bar{\mathbf{B}}_1 \langle e^{-ip_*^{(1)} \eta(x_3-d)} \rangle \bar{\mathbf{q}}_1^\infty - \bar{\mathbf{B}}_1 \langle e^{-ip_*^{(1)} \eta x_3} \rangle \bar{\mathbf{q}}_1, \\ \tilde{\mathbf{s}}_1(y_1, y_2, x_3) &= -\bar{\mathbf{C}}_1 \langle e^{-ip_*^{(1)} \eta(x_3-d)} \rangle \bar{\mathbf{q}}_1^\infty - \bar{\mathbf{C}}_1 \langle e^{-ip_*^{(1)} \eta x_3} \rangle \bar{\mathbf{q}}_1.\end{aligned}\quad (32)$$

For $0 \leq x_3 < d$ (in material 1):

$$\begin{aligned}\tilde{\mathbf{u}}_1(y_1, y_2, x_3) &= i\eta^{-1} \mathbf{A}_1 \langle e^{-ip_*^{(1)} \eta(x_3-d)} \rangle \mathbf{q}_1^\infty - i\eta^{-1} \bar{\mathbf{A}}_1 \langle e^{-ip_*^{(1)} \eta x_3} \rangle \bar{\mathbf{q}}_1, \\ \tilde{\mathbf{t}}_1(y_1, y_2, x_3) &= \mathbf{B}_1 \langle e^{-ip_*^{(1)} \eta(x_3-d)} \rangle \mathbf{q}_1^\infty - \bar{\mathbf{B}}_1 \langle e^{-ip_*^{(1)} \eta x_3} \rangle \bar{\mathbf{q}}_1, \\ \tilde{\mathbf{s}}_1(y_1, y_2, x_3) &= \mathbf{C}_1 \langle e^{-ip_*^{(1)} \eta(x_3-d)} \rangle \mathbf{q}_1^\infty - \bar{\mathbf{C}}_1 \langle e^{-ip_*^{(1)} \eta x_3} \rangle \bar{\mathbf{q}}_1.\end{aligned}\quad (33)$$

For $x_3 < 0$ (in material 2):

$$\begin{aligned}\tilde{\mathbf{u}}_2(y_1, y_2, x_3) &= i\eta^{-1} \mathbf{A}_2 \langle e^{-ip_*^{(2)} \eta x_3} \rangle \mathbf{q}_2, \\ \tilde{\mathbf{t}}_2(y_1, y_2, x_3) &= \mathbf{B}_2 \langle e^{-ip_*^{(2)} \eta x_3} \rangle \mathbf{q}_2, \\ \tilde{\mathbf{s}}_2(y_1, y_2, x_3) &= \mathbf{C}_2 \langle e^{-ip_*^{(2)} \eta x_3} \rangle \mathbf{q}_2,\end{aligned}\quad (34)$$

where again, subscripts 1 and 2 denote the quantities in materials 1 and 2, respectively, and

$$\mathbf{q}_1^\infty = \mathbf{A}_1^T \mathbf{f}. \quad (35)$$

The complex vectors $\bar{\mathbf{q}}_1$ and \mathbf{q}_2 in Eqs. (32)–(34) are determined by

$$\begin{aligned}\bar{\mathbf{q}}_1 &= \mathbf{G}_1 \langle e^{ip_*^{(1)} \eta d} \rangle \mathbf{A}_1^T \mathbf{f}, \\ \mathbf{q}_2 &= \mathbf{G}_2 \langle e^{ip_*^{(1)} \eta d} \rangle \mathbf{A}_1^T \mathbf{f},\end{aligned}\quad (36)$$

$$\begin{aligned}\mathbf{G}_1 &= -\bar{\mathbf{A}}_1^{-1} (\bar{\mathbf{M}}_1 + \mathbf{M}_2)^{-1} (\mathbf{M}_1 - \mathbf{M}_2) \mathbf{A}_1, \\ \mathbf{G}_2 &= \mathbf{A}_2^{-1} (\bar{\mathbf{M}}_1 + \mathbf{M}_2)^{-1} (\mathbf{M}_1 + \bar{\mathbf{M}}_1) \mathbf{A}_1,\end{aligned}\quad (37)$$

where \mathbf{M}_α are the extended impedance tensors defined as

$$\mathbf{M}_\alpha = -i\mathbf{B}_\alpha \mathbf{A}_\alpha^{-1} \quad (\alpha = 1, 2). \quad (38)$$

Eqs. (32)–(34) are the anisotropic piezoelectric bimaterial Green's displacements and stresses in the Fourier transformed domain. Similar to the purely elastic bimaterial case, several important features pertaining to these Green's functions are highlighted below.

1. For the solutions in material 1 ($x_3 > 0$), the first terms in Eqs. (32) and (33) (with a superscript ∞) are the Green's function in the transformed domain for the anisotropic piezoelectric full space. The inverse of this Green's function, i.e., the physical-domain solutions, has been developed recently by Pan and Tonon [2] in an explicit form. Therefore, the Fourier inverse transform needs to be carried out only for the second terms of the solutions, which are similar to the complementary part of Mindlin's solution [14]. This observation is critical in that the singularities involved in the physical-domain bimaterial Green's function actually appear only in the full-space Green's function. Since the latter function has an explicit-form representation, such singularities can be evaluated easily. Thus, the complementary part of the bimaterial Green's function is regular everywhere in its assigned region with the only exception of $x_3 = d = 0$. However, this special case can be addressed in a similar way as for the purely elastic case [1, Appendix].
2. The current anisotropic piezoelectric bimaterial Green's functions can be reduced to the uncoupled purely elastic and purely electric solutions by setting the piezoelectric coefficients e_{ijk} equal to 0.
3. When the material properties in materials 1 and 2 are identical, $\mathbf{G}_1 = \mathbf{0}$ and $\mathbf{G}_2 = \mathbf{I}$, the expressions of the coefficients in Eq. (36) are reduced to

$$\begin{aligned}\bar{\mathbf{q}}_1 &= \mathbf{0}, \\ \mathbf{q}_2 &= \langle e^{ip_*^{(1)}\eta d} \rangle \mathbf{A}_1^T \mathbf{f}.\end{aligned}\tag{39}$$

Thus, the bimaterial Green's functions are reduced automatically to the solutions in the full space.

4. When $d \rightarrow 0^+$, the solutions in the region $0 \leq x_3 < d$ disappear, and the remaining Green's functions are reduced to the interfacial Green's functions with an extended point force applied at the interface of material 1.
5. Eqs. (32)–(34) can also be reduced to the half-space Green's functions by ignoring Eq. (34) (i.e., solutions in material 2) and letting $\mathbf{B}_2 = \mathbf{0}$. In this case, \mathbf{G}_1 in Eq. (37) is simplified to

$$\mathbf{G}_1 = \bar{\mathbf{B}}_1^{-1} \mathbf{B}_1.\tag{40}$$

6. Bimaterial Greens functions in the physical domain

Having obtained Green's functions in the transformed domain, we now apply the inverse Fourier transform to Eqs. (32)–(34). To handle the double infinite integrals, the polar coordinate transform is introduced so that the infinite integral with respect to the radial variable can be carried out exactly [1]. Thus, the final bimaterial Green's functions in the physical domain can be expressed in terms of regular line integrals over $[0, 2\pi]$. In the following, we will use only the

extended displacement solution in region $x_3 > d$ of material 1 to illustrate the derivation, and then list the final results for other Green's functions.

Applying the Fourier inverse transform, the extended Green's displacement in Eq. (32) becomes

$$\begin{aligned} \mathbf{u}_1(x_1, x_2, x_3) = & -\frac{i}{4\pi^2} \int \int \{ \eta^{-1} \bar{\mathbf{A}}_1 \langle e^{-i\bar{p}_*^{(1)} \eta(x_3-d)} \rangle \bar{\mathbf{q}}_1^\infty e^{-i(x_1 y_1 + x_2 y_2)} \} dy_1 dy_2 \\ & -\frac{i}{4\pi^2} \int \int \{ \eta^{-1} \bar{\mathbf{A}}_1 \langle e^{-i\bar{p}_*^{(1)} \eta x_3} \rangle \bar{\mathbf{q}}_1 e^{-i(x_1 y_1 + x_2 y_2)} \} dy_1 dy_2. \end{aligned} \quad (41)$$

The first integral in Eq. (41) corresponds to the full-space extended Green's displacement that is available in an explicit form [2]. Consequently, the inverse transform needs to be carried out only for the second regular integral, or the complementary part. The singularities involved in the bimaterial Green's function appear only in the full-space solution that can be evaluated easily because of its explicit-form expression. Denoting the full-space Green's function by $\mathbf{u}_1^\infty(x_1, x_2, x_3)$ and introducing a polar coordinate transform consistent with the one defined in Eq. (16), i.e.,

$$\begin{aligned} y_1 &= \eta \cos \theta, \\ y_2 &= \eta \sin \theta. \end{aligned} \quad (42)$$

Then Eq. (41), also with use of (36a), becomes [1]

$$\begin{aligned} \mathbf{u}_1(x_1, x_2, x_3) = & \mathbf{u}_1^\infty(x_1, x_2, x_3) \\ & -\frac{i}{4\pi^2} \left[\int_0^{2\pi} d\theta \int_0^\infty \bar{\mathbf{A}}_1 \langle e^{-i\bar{p}_*^{(1)} \eta x_3} \rangle \mathbf{G}_1 \langle e^{i\bar{p}_*^{(1)} \eta d} \rangle e^{-i\eta(x_1 \cos \theta + x_2 \sin \theta)} \mathbf{A}_1^T d\eta \right] \mathbf{f}. \end{aligned} \quad (43)$$

Since the matrices \mathbf{A}_1 and \mathbf{G}_1 are independent of the radial variable η , the integral with respect to η can actually be performed analytically. Assuming that $x_3 \neq 0$ or $d \neq 0$, Eq. (43) can be reduced to a compact form

$$\mathbf{u}_1(x_1, x_2, x_3) = \mathbf{u}_1^\infty(x_1, x_2, x_3) + \frac{1}{4\pi^2} \left[\int_0^{2\pi} \bar{\mathbf{A}}_1 \mathbf{G}_u^{(1)} \mathbf{A}_1^T d\theta \right] \mathbf{f}, \quad (44)$$

where

$$(\mathbf{G}_u^{(1)})_{IJ} = \frac{(\mathbf{G}_1)_{IJ}}{-\bar{p}_I^{(1)} x_3 + p_J^{(1)} d - (x_1 \cos \theta + x_2 \sin \theta)}. \quad (45)$$

Using a similar procedure, other bimaterial Green's functions can be derived and the results are listed below:

$$\begin{aligned} \mathbf{t}_1(x_1, x_2, x_3) &= \mathbf{t}_1^\infty(x_1, x_2, x_3) + \frac{1}{4\pi^2} \left[\int_0^{2\pi} \bar{\mathbf{B}}_1 \mathbf{G}_t^{(1)} \mathbf{A}_1^T d\theta \right] \mathbf{f}, \\ \mathbf{s}_1(x_1, x_2, x_3) &= \mathbf{s}_1^\infty(x_1, x_2, x_3) + \frac{1}{4\pi^2} \left[\int_0^{2\pi} \bar{\mathbf{C}}_1 \mathbf{G}_t^{(1)} \mathbf{A}_1^T d\theta \right] \mathbf{f}, \end{aligned} \tag{46}$$

$$\begin{aligned} \mathbf{u}_2(x_1, x_2, x_3) &= -\frac{1}{4\pi^2} \left[\int_0^{2\pi} \mathbf{A}_2 \mathbf{G}_u^{(2)} \mathbf{A}_1^T d\theta \right] \mathbf{f}, \\ \mathbf{t}_2(x_1, x_2, x_3) &= -\frac{1}{4\pi^2} \left[\int_0^{2\pi} \mathbf{B}_2 \mathbf{G}_t^{(2)} \mathbf{A}_1^T d\theta \right] \mathbf{f}, \\ \mathbf{s}_2(x_1, x_2, x_3) &= -\frac{1}{4\pi^2} \left[\int_0^{2\pi} \mathbf{C}_2 \mathbf{G}_t^{(2)} \mathbf{A}_1^T d\theta \right] \mathbf{f}. \end{aligned} \tag{47}$$

In Eqs. (46) and (47), $\mathbf{t}_1^\infty(x_1, x_2, x_3)$ and $\mathbf{s}_1^\infty(x_1, x_2, x_3)$ are Green’s stresses in the full space and

$$(\mathbf{G}_t^{(1)})_{IJ} = \frac{(\mathbf{G}_1)_{IJ}}{[-p_I^{(1)} x_3 + p_J^{(1)} d - (x_1 \cos \theta + x_2 \sin \theta)]^2}, \tag{48}$$

$$(\mathbf{G}_u^{(2)})_{IJ} = \frac{(\mathbf{G}_2)_{IJ}}{-p_I^{(2)} x_3 + p_J^{(1)} d - (x_1 \cos \theta + x_2 \sin \theta)}, \tag{49}$$

$$(\mathbf{G}_t^{(2)})_{IJ} = \frac{(\mathbf{G}_2)_{IJ}}{[-p_I^{(2)} x_3 + p_J^{(1)} d - (x_1 \cos \theta + x_2 \sin \theta)]^2}. \tag{50}$$

Therefore, the complementary part of the extended bimaterial Green’s displacements and stresses can be expressed in terms of regular line integrals over $[0, 2\pi]$. With regard to these physical-domain bimaterial Green’s functions, Eqs. (44), (46) and (47), the following important observations similar to the purely elastic counterpart can be made:

1. In deriving the results, we have assumed that the extended point force (source point) is located at $(0, 0, d)$. For an extended force located at (x_1^0, x_2^0, d) , the variables x_1 and x_2 in the above expressions need to be replaced by $x_1 - x_1^0$ and $x_2 - x_2^0$, respectively.
2. Similar to the procedures made on the transformed-domain Green’s functions, the physical-domain Green’s functions presented here can be reduced to the half-space, interfacial, and homogeneous Green’s functions by a suitable substitution of the involved vectors and matrices. Furthermore, the uncoupled purely elastic and purely electric solutions can be obtained by letting the piezoelectric coefficients e_{ijk} equal to 0.
3. For the complementary part of the solution in material 1 and the solution in material 2, the dependence of the solutions on the field point (x_1, x_2, x_3) and source point (x_1^0, x_2^0, d) appears only through matrices $\mathbf{G}_u^{(1)}$, $\mathbf{G}_t^{(1)}$, $\mathbf{G}_u^{(2)}$, and $\mathbf{G}_t^{(2)}$ as defined in Eqs. (45),(48)–(50). Therefore, the derivatives of the bimaterial Green’s functions with respect to either the field or source point can be exactly carried out under the integral sign. These derivatives are required in the bound-

ary integral equation method for the internal stress and fracture analyses in piezoelectric bimaterial solids.

4. The piezoelectric bimaterial Green's functions for the extended displacements and stresses are inversely proportional to, respectively, a linear and quadratic combination of the field and source coordinates. These features resemble the behavior of the full-space extended Green's displacement ($\propto 1/r$) and stress ($\propto 1/r^2$) where r is the distance between the source and field points.
5. The integrals in Eqs. (44), (46) and (47) for performing the complementary part of Green's functions are regular and thus can be easily carried out by a standard numerical integral method such as the Gauss quadrature.
6. In deriving the physical-domain bimaterial Green's functions, $x_3 \neq 0$ or $d \neq 0$ has been assumed. For the special case of $x_3 = d = 0$, i.e., both the field and source points are located on the interface for the bimaterial case or on the surface for the half-space case, Green's functions presented above need to be modified. Again, this special case can be treated in a similar way as for the purely elastic case [1, Appendix]. In particular, a real form line-integral expression of the extended displacement on the surface of an anisotropic piezoelectric half space can be derived in terms of the generalized Barnett–Lothe tensors \mathbf{S} , \mathbf{H} and \mathbf{L} for the piezoelectric materials, a counterpart of the elastic solution derived by Barnett and Lothe [17].

7. Numerical examples

Before using the present solutions to the half space and bimaterial cases, we validated our formulation for the following special cases:

1. A half-space case where the extended traction-free conditions must be satisfied.
2. An artificial bimaterial full-space case with identical material properties in materials 1 and 2 where the present solution must reduce to the full-space Green's function solutions.
3. The uncoupled case where the current solutions must reduce to the purely elastic bimaterial Green's functions [1].

Two types of piezoelectric materials are selected for the numerical studies: Material A is transversely isotropic [18], and material B is anisotropic [15], with the material properties being given in Eqs. (51a)–(52c), respectively:

Material A

$$[C] = \begin{bmatrix} 1.39 & 0.778 & 0.743 & 0 & 0 & 0 \\ 0.778 & 1.39 & 0.743 & 0 & 0 & 0 \\ 0.743 & 0.743 & 1.15 & 0 & 0 & 0 \\ 0 & 0 & 0 & 0.256 & 0 & 0 \\ 0 & 0 & 0 & 0 & 0.256 & 0 \\ 0 & 0 & 0 & 0 & 0 & 0.306 \end{bmatrix} (10^{11} \text{ N/m}^2), \quad (51a)$$

$$[e] = \begin{bmatrix} 0 & 0 & 0 & 0 & 12.7 & 0 \\ 0 & 0 & 0 & 12.7 & 0 & 0 \\ -5.2 & -5.2 & 15.1 & 0 & 0 & 0 \end{bmatrix} (\text{C/m}^2), \quad (51b)$$

$$[\varepsilon] = \begin{bmatrix} 0.64605 & 0 & 0 \\ 0 & 0.64605 & 0 \\ 0 & 0 & 0.561975 \end{bmatrix} (10^{-8} \text{ C/Vm}). \quad (51c)$$

Material B

$$[C] = \begin{bmatrix} 0.8674 & -0.0825 & 0.2715 & -0.0366 & 0 & 0 \\ -0.0825 & 1.2977 & -0.0742 & 0.057 & 0 & 0 \\ 0.2715 & -0.0742 & 1.0283 & 0.0992 & 0 & 0 \\ -0.0366 & 0.057 & 0.0992 & 0.3861 & 0 & 0 \\ 0 & 0 & 0 & 0 & 0.6881 & 0.0253 \\ 0 & 0 & 0 & 0 & 0.0253 & 0.6881 \end{bmatrix} (10^{11} \text{ N/m}^2), \quad (52a)$$

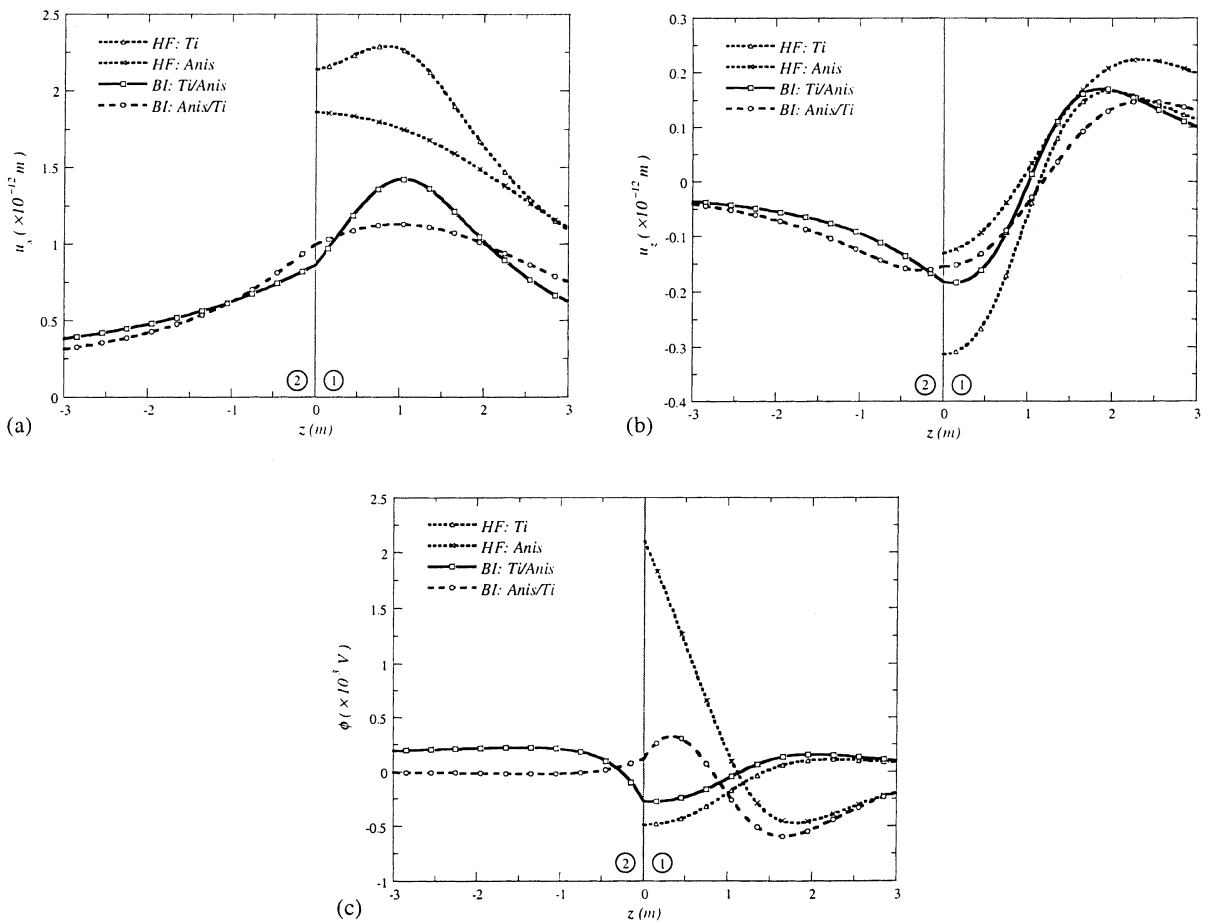


Fig. 2. Extended Green's displacements due to a point force in the x-direction. u_x in (a), u_z in (b), and ϕ in (c).

$$[e] = \begin{bmatrix} 0.171 & -0.152 & -0.0187 & 0.067 & 0 & 0 \\ 0 & 0 & 0 & 0 & 0.108 & -0.095 \\ 0 & 0 & 0 & 0 & -0.0761 & 0.067 \end{bmatrix} (\text{C/m}^2), \quad (52b)$$

$$[\varepsilon] = \begin{bmatrix} 0.3921 & 0 & 0 \\ 0 & 0.3982 & 0.0086 \\ 0 & 0.0086 & 0.4042 \end{bmatrix} (10^{-10} \text{ C/Vm}). \quad (52c)$$

In these equations, $[C]$ and $[e]$ represent the elastic constants and piezoelectric coefficients in a contracted matrix notation, respectively. It is observed that while the elastic constants for these two materials have the same order of magnitude, the piezoelectric and dielectric constants in the anisotropic material are, respectively, two orders of magnitude smaller than those in the transversely isotropic material. It is further noted that since the difference in the magnitudes of $[C]$ and

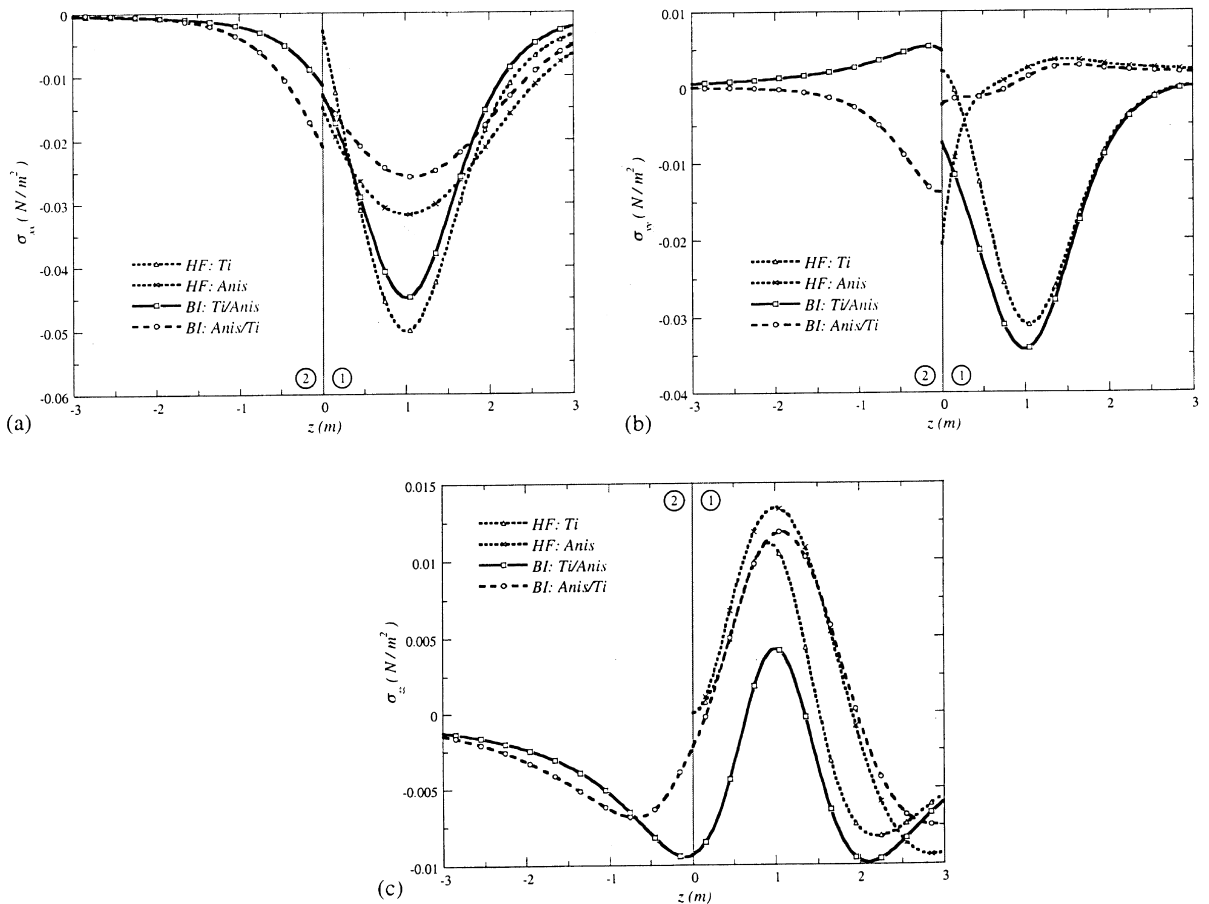


Fig. 3. Green's normal stresses due to a point force in the x -direction. σ_{xx} in (a), σ_{yy} in (b), and σ_{zz} in (c).

[e] is substantial, a suitable normalization is introduced when calculating Green’s functions using the present formulation.

With these material properties, we have been able to check our formulation for the three special cases. Indeed, for a half-space case, the traction-free boundary conditions were satisfied exactly. This can also be observed from the numerical examples given below. As the second check of our formulation, we calculated Green’s functions in an artificially bimaterial full space. From our derivations given above, we noted that when the source and field points are not at the same half space, Green’s functions contain only the complementary part. These Green’s functions have been calculated for several pairs of source and field points, and the results are exactly the same as those obtained based on the full-space Green’s functions [2,6]. Finally, assuming the piezoelectric coefficients [e] to be zero, we have been able to use our formulation to derive the same purely elastic bimaterial Green’s functions as presented by Pan and Yuan [1].

Having tested our Green’s functions for the special cases, we now present the numerical results for the extended Green’s displacements and stresses in a half space and bimaterial full space, with

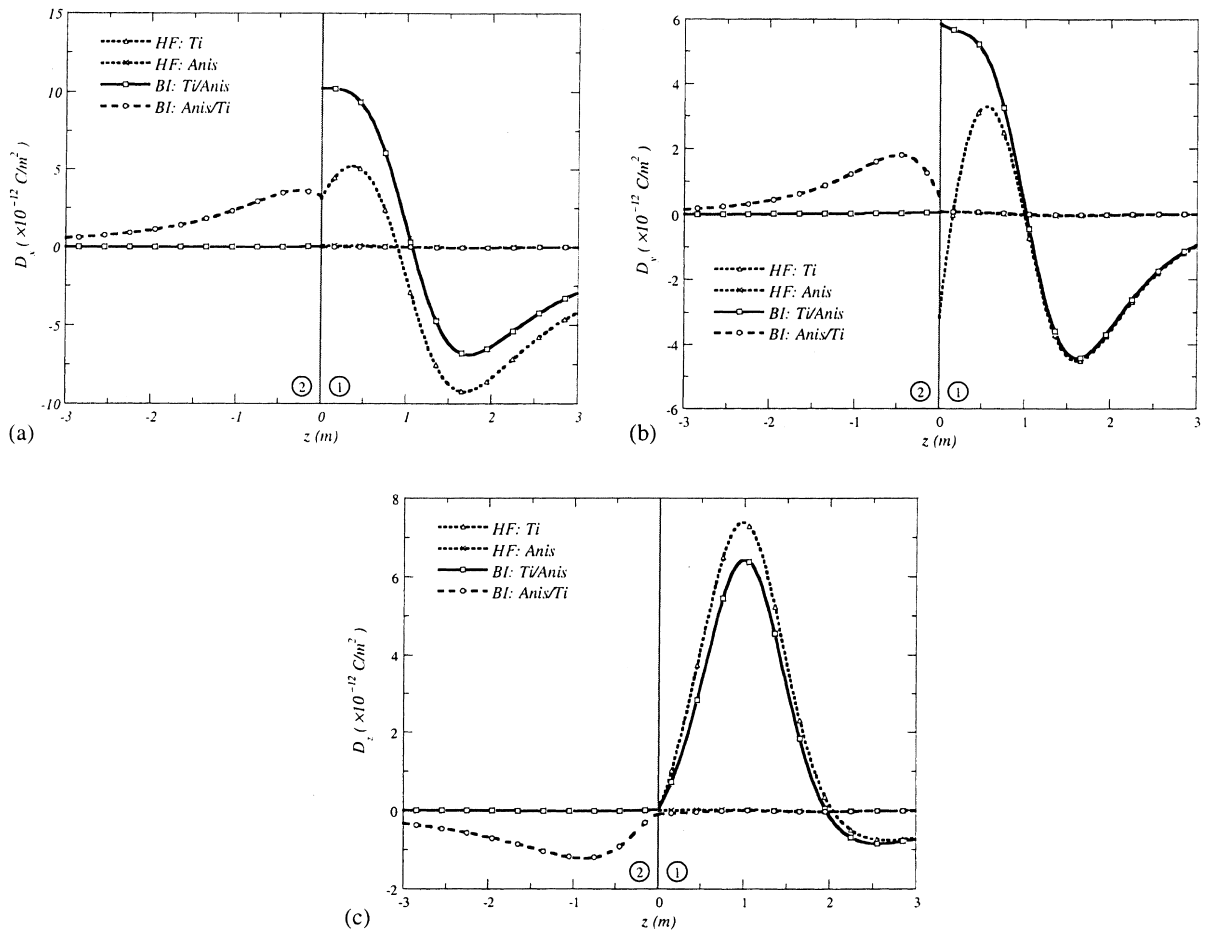


Fig. 4. Green’s electric displacements due to a point force in the x -direction. D_x in (a), D_y in (b), and D_z in (c).

material properties being either transversely isotropic (material A) or anisotropic (material B). Four cases are considered below:

Case I: A half space with transverse isotropy (HF: Ti).

Case II: A half space with anisotropy (HF: Anis).

Case III: Bimaterials with transverse isotropy in material 1 and anisotropy in material 2 (BI: Ti/Anis).

Case IV: Bimaterials with anisotropy in material 1 and transverse isotropy in material 2 (BI: Anis/Ti).

The extended Green’s displacements and normal stresses are presented in Figs. 2–4, Figs. 5–7 and Figs. 8–10, respectively, for a x - (or x_1 -) direction point force, z -direction (or x_3 -) point force, and a negative point electric charge. In these figures, a point force of 1 N/m^3 (or a negative point charge of 1 C/m^3) is applied at $(0, 0, 1 \text{ m})$. The extended displacements and stresses are plotted at field points $(1 \text{ m}, 1 \text{ m}, z)$ with z varying from 0 to 3 m for Cases I and II, and from -3 to 3 m for Cases III and IV.

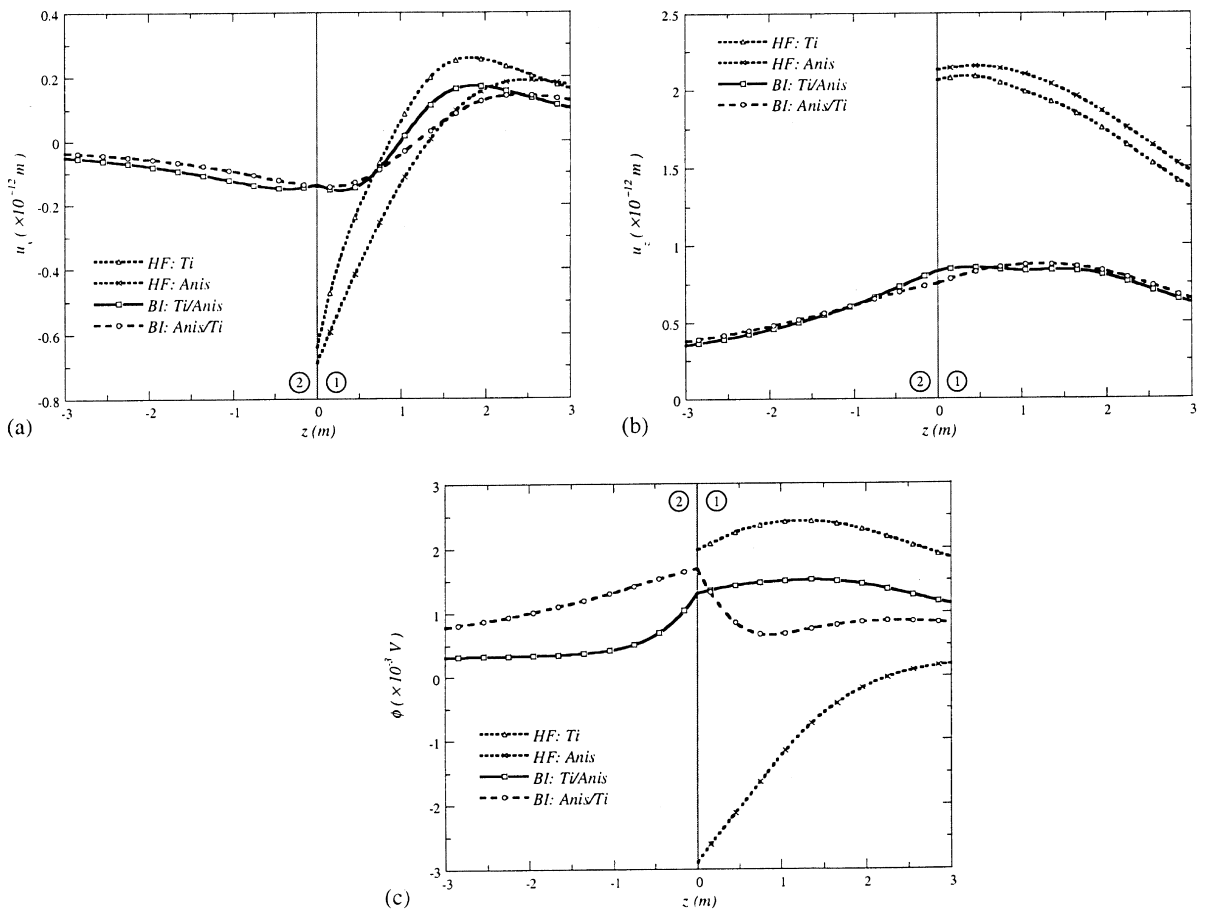


Fig. 5. Extended Green’s displacements due to a point force in the z -direction. u_x in (a), u_z in (b), and ϕ in (c).

From Figs. 2–4, and Figs. 8–10, we observed that under the x -direction point force and a negative point charge, the variation of the extended displacements and stresses in material 1 are similar to each other for Cases I and III, and for Cases II and IV, respectively. In other words, they are similar to each other if their piezoelectric properties are the same in material 1, despite whether the domain is half space or bimaterial. This behavior is more obvious when the field point is relatively far away from the source and the plane $x_3 = 0$ (or $z = 0$). This implies that under the horizontal point force (x - or y -direction) or point charge, Green’s functions are more materially dominant. Under the vertical point force (z -direction), however, Green’s functions are similar to each other for Cases I and II (half space) and for Cases III and IV (bimaterials), respectively. In other words, Green’s functions due to z -direction point force are more likely regionally dominant.

Another interesting feature of Green’s functions is associated with the response of the electric displacements. It is observed that (Figs. 4, 7, and 10) for the given material properties all the

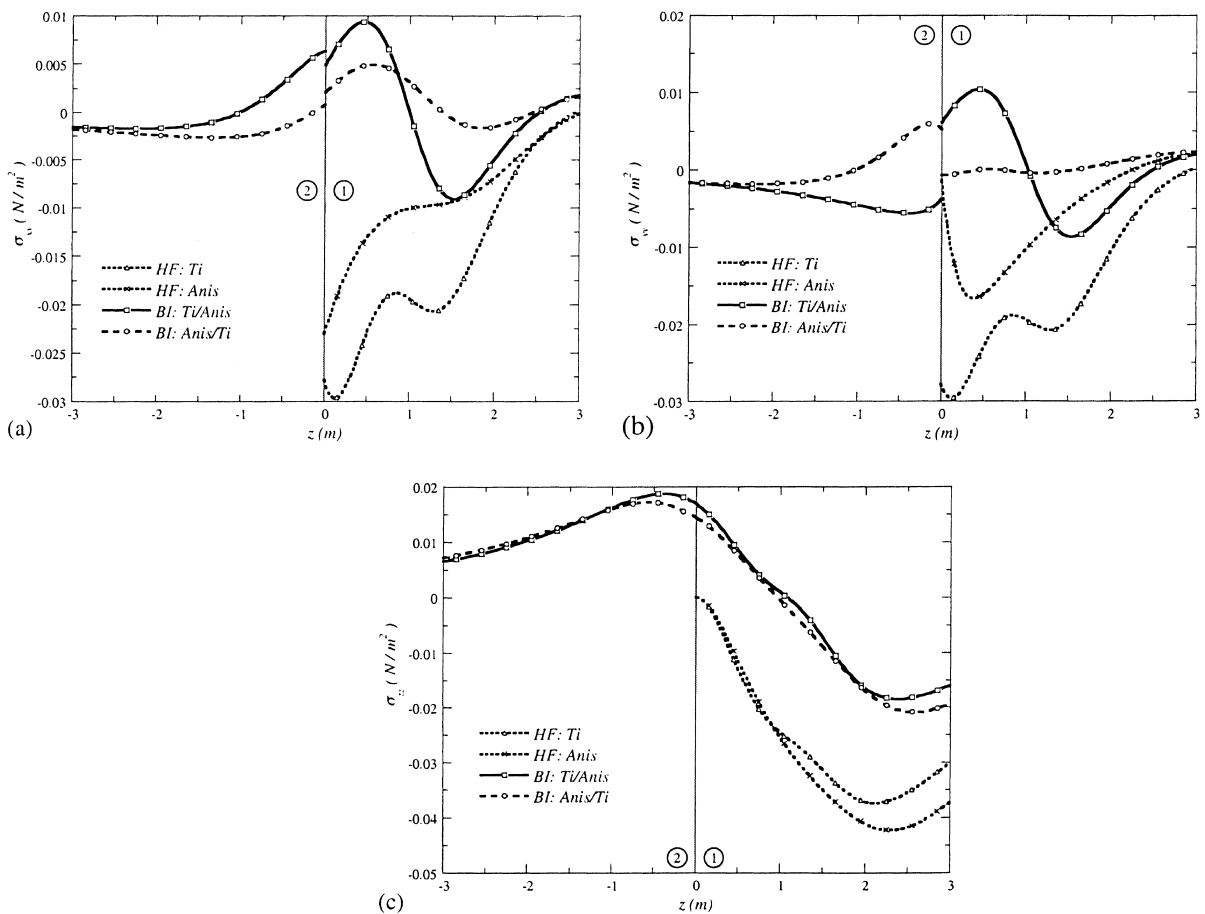


Fig. 6. Green’s normal stresses due to a point force in the z -direction. σ_{xx} in (a), σ_{yy} in (b), and σ_{zz} in (c).

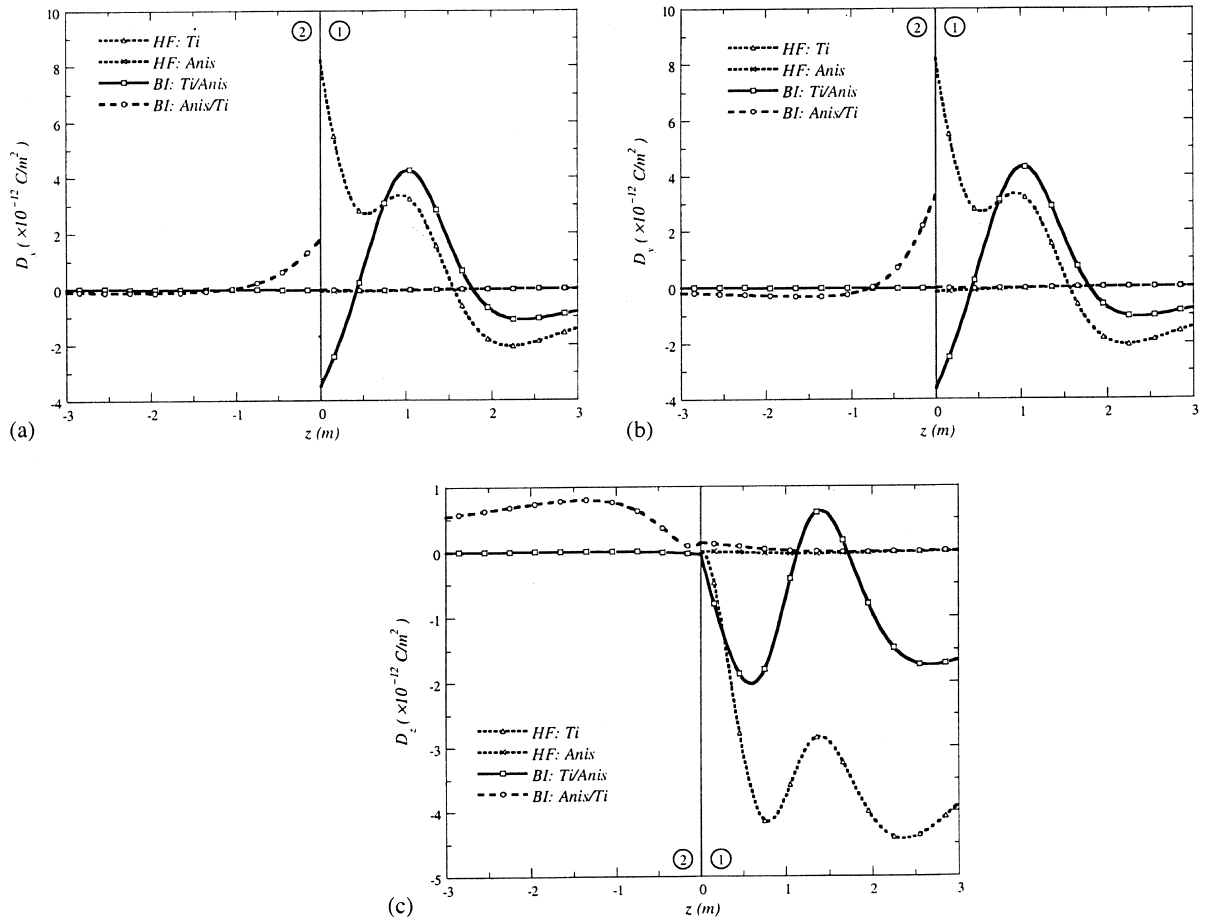


Fig. 7. Green's electric displacements due to a point force in the z -direction. D_x in (a), D_y in (b), and D_z in (c).

electric displacements in the region with anisotropic material properties are about two orders smaller (10^{-2}) than those in the transversely isotropic region. Therefore, the electric displacements in the anisotropic region are negligible compared to those in the transversely isotropic region (although they appear as straight lines in Figs. 4, 7, and 10 in the anisotropic region, they should not be misunderstood as zero values). This is due to the fact that the piezoelectric and dielectric constants in the anisotropic region are, respectively, two orders smaller than those in the transversely isotropic region.

A final feature of Green's functions is related to the electric potential due to a negative point charge (Fig. 8c). It is interesting that only in the source region with anisotropic material properties, can the electric potential variation be observed. For all other cases, the electric potentials are on the order of 10^7 V, two orders smaller (the straight lines should not be mistreated as zeros) than those in the source region with anisotropic material properties. This feature again is directly associated to the material properties we have chosen.

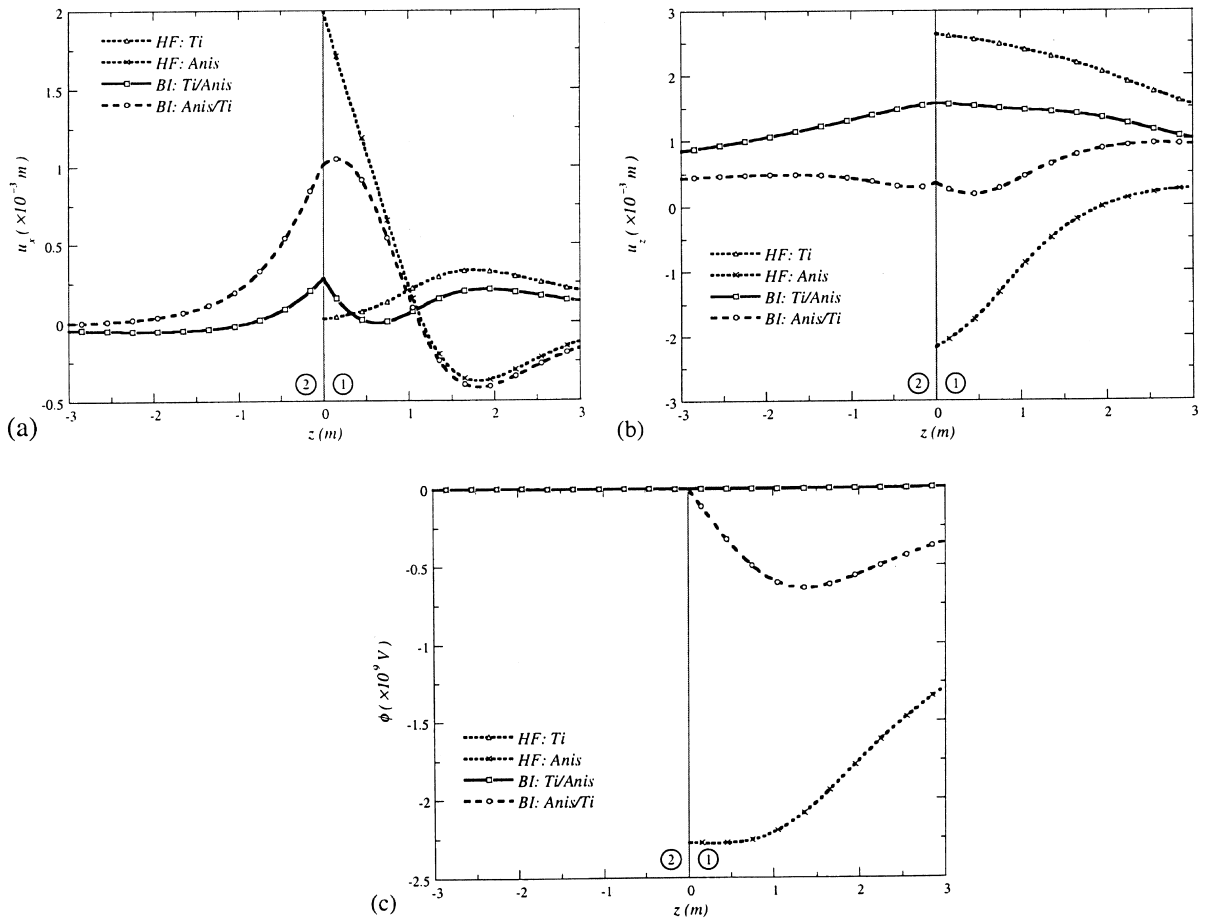


Fig. 8. Extended Green's displacements due to a negative point charge. u_x in (a), u_z in (b), and ϕ in (c).

8. Conclusions

In this paper, three-dimensional Green's functions of point forces and point charge in anisotropic piezoelectric bimetals are derived in terms of a regular line integral. We first derived the transformed-domain Green's functions in exact closed forms using the Stroh formalism. In order to obtain the physical domain Green's functions, the Fourier inverse transform using a polar coordinate system is proposed to reduce the double infinite integrals to a finite line integral over $[0, 2\pi]$. Mindlin's superposition method [14] is also employed to handle the singularities in the piezoelectric bimaterial Green's functions so that the involved singularities appear only in the full-space Green's function that can be evaluated accurately using its explicit form expression (without numerical integral!). Therefore, the final physical piezoelectric bimaterial Green's functions are expressed as a sum of the explicit full-space Green's function and a complementary part. The complementary part of the bimaterial Green's functions is represented in terms of a regular line integral that can be easily carried out by the regular numerical Gauss quadrature. In addition,

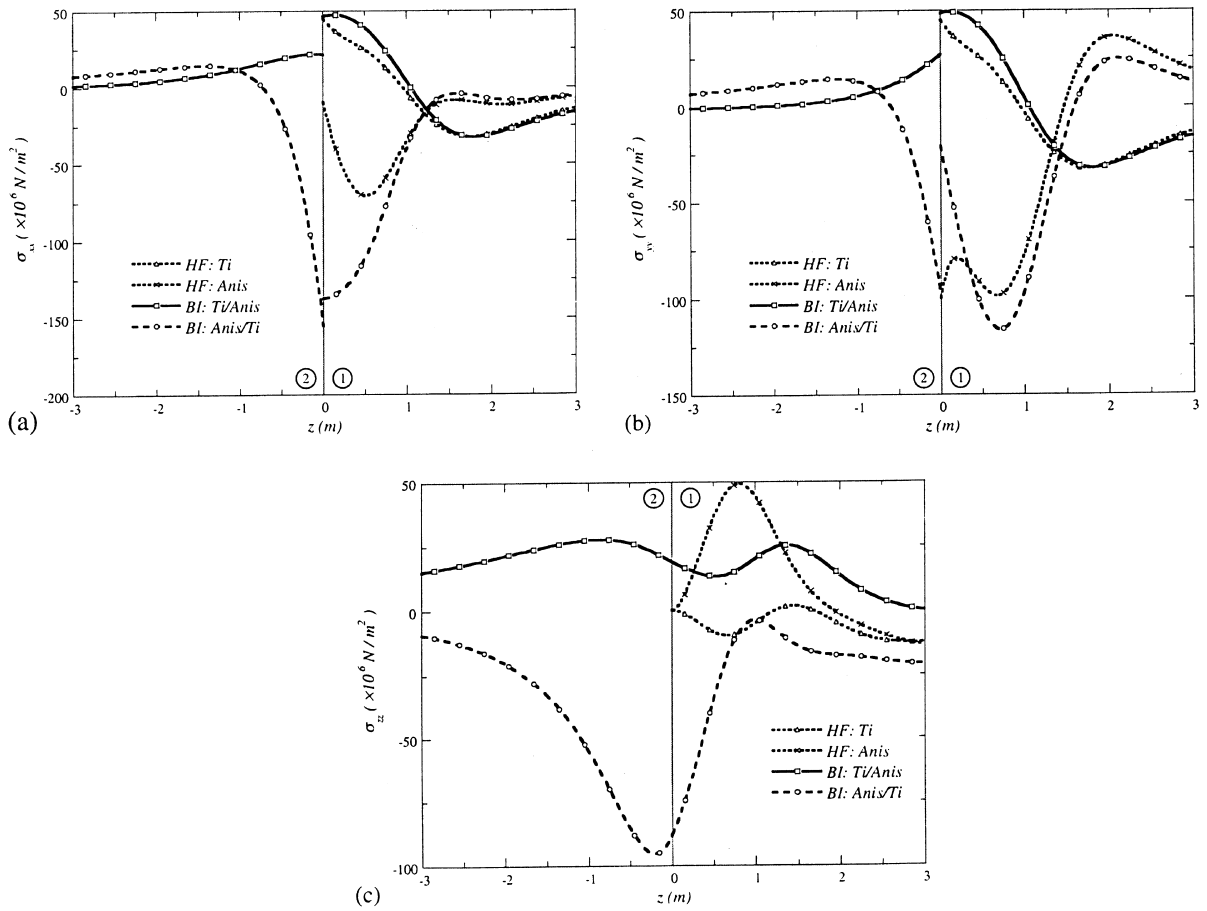


Fig. 9. Green's normal stresses due to a negative point charge. σ_{xx} in (a), σ_{yy} in (b), and σ_{zz} in (c).

derivatives of the complementary part of Green's functions with respect to either the source or field point can be carried out exactly under the line integral. Some important features related to the piezoelectric bimaterial Green's functions and their reduction to special cases have been discussed.

Numerical examples are also presented for both half-space and bimaterial cases with transversely isotropic and anisotropic material properties. The responses of Green's functions for different half-space and bimaterial cases due to different types of point sources are discussed. It is observed that some of these Green's functions are material-dependent (i.e., in the source region with the same material properties, the Green's functions behave similarly for both the half-space and bimaterial cases), others are case-dependent (i.e., the Green's functions behave similarly for a half-space case or bimaterial case despite whether the material property is transversely isotropic or anisotropic). Another interesting feature, although strongly tied to the selected material properties, is associated with the responses of the Green's electric displacements where the electric displacements in the anisotropic region are negligible compared to those in the transversely isotropic region.

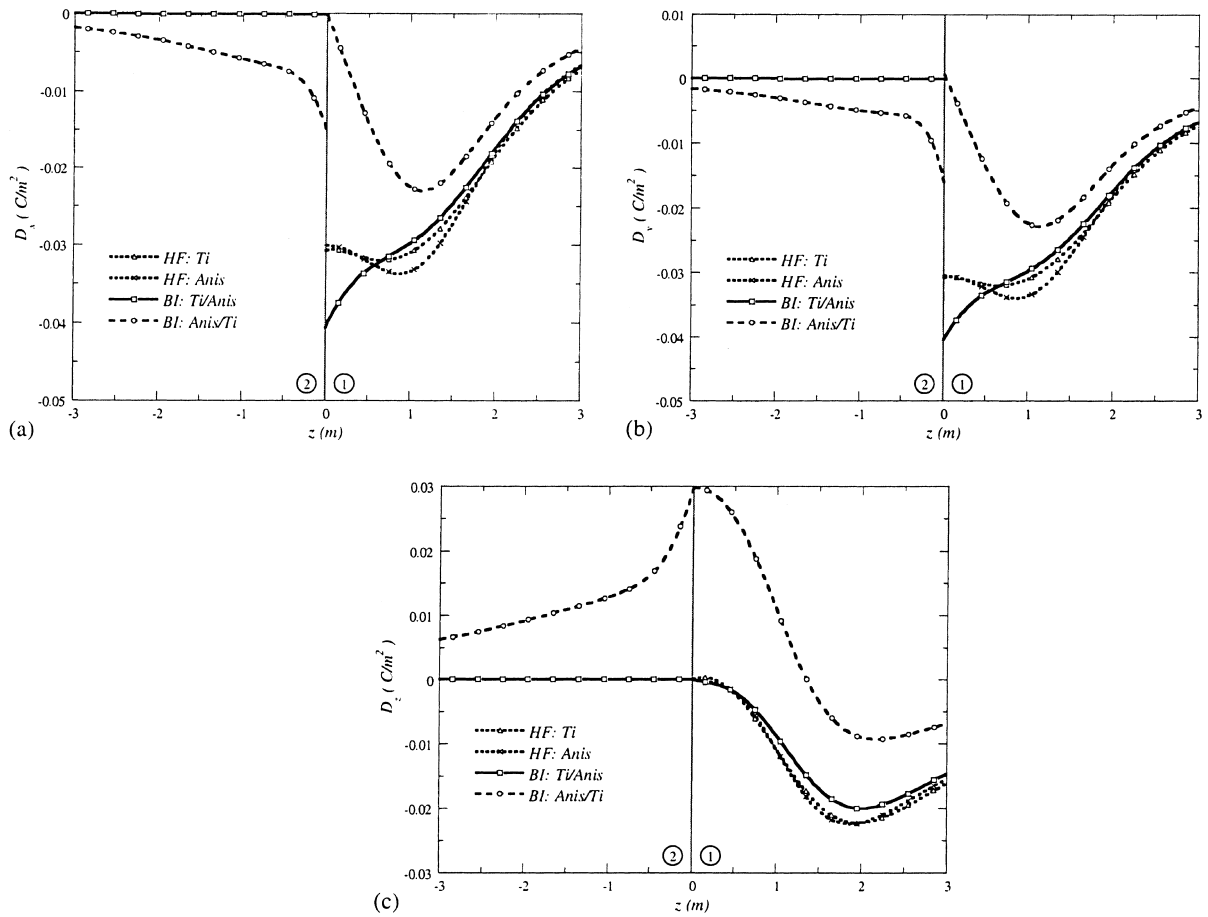


Fig. 10. Green's electric displacements due to a negative point charge. D_x in (a), D_y in (b), and D_z in (c).

Acknowledgements

This project was supported by the AFOSR under grant no. F33615-97-C-5089 with Dr. Richard B. Hall as the program monitor. The authors would also like to thank the support from the Structures Technology, Inc. to carry out this research, and Dr. Gary Cai of Structures Technology for some helpful discussions.

References

- [1] E. Pan, F.G. Yuan, Three-dimensional Green's functions in anisotropic bimerials, *Int. J. Solids Struct.*, 2000 (in press).
- [2] E. Pan, F. Tonon, Three-dimensional Green's functions in anisotropic piezoelectric solids, *Int. J. Solids Struct.* 37 (2000) 943–958.
- [3] D.M. Barnett, J. Lothe, Dislocations and line charges in anisotropic piezoelectric insulators, *Phys. Stat. Sol. (B)* 67 (1975) 105–111.

- [4] T.C.T. Ting, *Anisotropic Elasticity*, Oxford University Press, Oxford, 1996.
- [5] E. Pan, A BEM analysis of fracture mechanics in 2D anisotropic piezoelectric solids, *Eng. Anal. with Boundary Elements* 23 (1999) 67–76.
- [6] M.L. Dunn, H.A. Wienecke, Green's functions for transversely isotropic piezoelectric solids, *Int. J. Solids Struct.* 33 (1996) 4571–4581.
- [7] M.L. Dunn, H.A. Wienecke, Half-space Green's functions for transversely isotropic piezoelectric solids, *J. Appl. Mech.* 66 (1999) 675–679.
- [8] H.J. Ding, B. Chen, J. Liang, On the general solutions for coupled equation for piezoelectric media, *Int. J. Solids Struct.* 33 (1996) 2283–2298.
- [9] H.J. Ding, B. Chen, J. Liang, On the Green's functions for two-phase transversely isotropic piezoelectric media, *Int. J. Solids Struct.* 34 (1997) 3041–3057.
- [10] H.J. Ding, Y. Chi, F. Guo, Solutions for transversely isotropic piezoelectric infinite body, semi-finite body and bimaterial infinite body subjected to uniform ring loading and charge, *Int. J. Solids Struct.* 36 (1999) 2613–2631.
- [11] D.M. Barnett, The precise evaluation of derivatives of the anisotropic elastic Green's functions, *Phys. Stat. Sol. B* 49 (1972) 741–748.
- [12] T. Chen, Green's functions and the non-uniform transformation problem in a piezoelectric medium, *Mech. Res. Comm.* 20 (1993) 271–278.
- [13] T. Chen, F.Z. Lin, Numerical evaluation of derivatives of the anisotropic piezoelectric Green's functions, *Mech. Res. Comm.* 20 (1993) 501–506.
- [14] R.D. Mindlin, Force at a point in the interior of a semi-infinite solid, *Physics* 7 (1936) 195–202.
- [15] H.F. Tiersten, *Linear Piezoelectric Plate Vibrations*, Plenum, New York, 1969.
- [16] Z. Suo, C.M. Kuo, D.M. Barnett, J.R. Willis, Fracture mechanics for piezoelectric ceramics, *J. Mech. Phys. Solids* 40 (1992) 739–765.
- [17] D.M. Barnett, J. Lothe, Line force loadings on anisotropic half spaces and wedges, *Physica Norvegica* 8 (1) (1975) 13–22.
- [18] M.L. Dunn, M. Taya, An analysis of piezoelectric composite materials containing ellipsoidal inhomogeneities, *Proc. R. Soc. Lond. A* 443 (1993) 265–287.